Combinatorial Optimization Systems Theory Prospected from Rotational Symmetry

VOLODYMYR RIZNYK
Department of Computer Aided Control Systems
Lviv Polytechnic National University
79013, Lviv-13, Stepan Bandera Str., 12
UKRAINE

Abstract: - Combinatorial optimization systems theory prospected from rotational symmetry involves techniques for improving the quality indices of engineering devices or systems with non-uniform structure (e.g., controllable cyber-physical objects) concerning transformation swiftness, position accuracy, and resolution, using designs based on extraordinary geometric properties and structural excellence of combinatorial conformations, namely the concept of Ideal Ring Bundles. Design techniques based on the underlying combinatorial theory provide configure one- and multidimensional systems with smaller amounts of elements than at present, while maintaining the other substantial operating characteristics of the systems.

Key-Words: - Cyclic group, Ideal Ring Bundle, torus reference system, GUS configuration, spatial perfection, manifold coordinates, vector data.

Received: July 22, 2023. Revised: May 21, 2024. Accepted: June 18, 2024. Published: July 23, 2024.

1 Introduction

Combinatorial optimization theory of systems [1] encompasses various scientific and technological fields such as software engineering, algorithm theory, operations research, machine learning, computational complexity theory, applied mathematics, and theoretical computer science. The classical combinatorial theory involves fundamental concepts of modern algebra and geometry, including difference sets in a finite group, finite projective planes, Hadamard matrices theory, cyclic incidence matrices, and the problematic of certain symmetrical balanced incomplete block designs, automorphisms of groups, and orthogonal Latin squares [2]. In paper [3], the study of some permutations helps discover unrelated classes. A multinomial function that describes a system with multi-input and multi-output systems has the coefficients for parameters [4]. Many original models, concepts, parallel algorithms, platforms, applications, and processing gears relate to improving the assessment of big data technology [5], [6], [7], artificial intelligence [8], [9], signal processing [10], [11], and radio engineering [12], advanced algorithms [13], [14], and cryptography [15]. The objective of this work is to test suitable sets of famous classes concerning a small subset of such functions based on the intelligence of rotational symmetry. The principle of symmetry and asymmetry is prevalent in nature and artificial environments, so it's crucial to consider rotational symmetry for the development of optimization systems theory in fundamental and applied research. This can be achieved through innovative methodologies based on the concept of Ideal Ring Bundles (IRBs) [16], which involves the idea of "perfect" multidimensional combinatorial constructions. This paper deals with techniques for improving the quality indices of controllable cyber-physical systems and vector processing, such as transformation speed, resolving ability, minimizing machinery memory, and computing resources, using designs based on the combinatorial optimization systems theory. Theoretical research into the combinatorial configuration's properties has led to a better understanding of the role of rotational symmetries in the theory. Modern combinatorial theory and system design connect with appropriate constructions such as manifolds [17], connecting algebra through geometry [18], and the Golden ratio [19], which involve the relationships of rotational symmetry spatial multidimensional configurations [16]. Symmetries and curvature structures are embedded in general relativity [20].

2 Optimum Combinatorial Structures

2.1 Optimum Combinatorial Sequences

A "well-ordered" sequence of distributed elements can be very useful in optimally solving various technological problems, leading to high profits.

2.1.1 Sums on a chain- ordered numbers

Let us compute all L sums of ordered-chain numbers in the n-stage sequence of positive integers $\{k_1, k_2, \ldots, k_n\}$, where the sums of connected sub-sequences of the sequence enumerate the set of integers from 1 to L. The maximum number of distinct sums on ordered-chain numbers is

$$L = n \cdot (n+1)/2 \qquad (1)$$

Another type of combinatorial construction is the use of ring structures.

2.2 Ring Numerical Structures

Let's consider a sequence of positive integers $\{k_1, k_2, ..., k_n\}$ arranged in a specific order such that k_n is followed by k_1, forming a chain structure. As we continue to add integers to this sequence, it eventually turns into a numerical ring structure with n stages. In contrast to an ordered chain, a ring numerical structure allows for a sum of connected sub-sequences to have any length from 1 to n–1 as its starting point, with the final sum including all n integers. Therefore, the maximum number of distinct sums S that can be obtained from the ring numerical structure is

$$S = n\,(n-1) + 1 \qquad (2)$$

Comparing the equations (1) and (2), easy to see that the number of sums S for connected terms in the ring topology is nearly double the number of sums L in the daisy-chain topology, for the same sequence of n terms.

$$\left.\begin{aligned}(1,0)+(1,1)&\equiv(0,1)\\(1,1)+(1,2)&\equiv(0,0)\\(1,2)+(1,0)&\equiv(0,2)\end{aligned}\right\}(\mathrm{mod}\,2, \mathrm{mod}\,3)$$

2.2.1 Ideal Ring Bundles

Ideal Ring Bundles are cyclic sequences of positive integers that form perfect partitions of a finite interval [1, S] of integers. The sums of consecutive sub-sequences of an Ideal Ring Bundle (IRB) enumerate the set of integers [1, S] exactly once. Here is an example of an IRB with n=5 and S=5(5–1) +1=21, namely {1,5,2,10,3}. To see this, we observe:

1=1	6=1+5	11=3+1+5+2	16=2+10+3+1
2=2	7=5+2	12=2+10	17=5+2+10
3=3	8=1+5+2	13=10+3	18=1+5+2+10
4=3+1	9=3+1+5	14=10+3+1	19=10+3+1+5
5=5	10=10	15=2+10+3	20=5+2+10+3
			21=1+5+2+10+3

$$\left.\begin{aligned}(1,0)\cdot(1,2)&\equiv(1,0)\\(1,1)\cdot(1,2)&\equiv(1,2)\\(1,2)\cdot(1,2)&\equiv(1,1)\end{aligned}\right\}(\mathrm{mod}\,2, \mathrm{mod}\,3)$$

We understand that each ring sum from 1 to S =21 occurs exactly once.

2.2.2 Relative of Ideal Ring Bundles to Rotational Symmetry

For a better understanding of the role of geometric structures in the combinatorial optimization systems theory, we regard Ideal Ring Bundles with informative parameters S and n as cyclic numerical relationships followed by equation (2) based on the idea of "generative" rotational symmetry of order S. Employing 21-fold rotational symmetry, the IRB can be configured using complementary asymmetries relations of geometric structure.

2.2.3 Two-Dimensional Ideal Ring Bundles

Let's consider a cyclic sequence of n -stages, denoted as $\{K_1, K_2, \ldots, K_i, \ldots, K_n\}$, $K_1 = (k_{11}, k_{12})$, $K_2 = (k_{21}, k_{22})$, ..., $K_i = (k_{i1}, k_{i2})$, ..., $K_n = (k_{n1}, k_{n2})$. This sequence consists of 2-stage (t=2) sub-sequences. We require that all two-dimensional modular vector sums (mod m_1, mod m_2) must form a two-dimensional coordinate grid of sizes $m_1 \times m_2$ over a toroidal surface, where $m_1 \cdot m_2 = S-1$. This configuration is known as the two-dimensional Ideal Ring Bundle (2-D IRB). Here are four variants of 2-D IRBs with parameters S =7, n = 3, $m_1 = n - 1 = 2$, and $m_2 = n = 3$:

(*a*) {(1,0),(1,1),(1,2)}; (*b*) {(0,1),(0,2),(1,0)};
(*c*) {(0,1),(0,2),(1,2)}; (*d*) {(0,1),(0,2),(1,1)}

The group {(1,0),(1,1),(1,2)} in two-dimensional IRB allows for addition and multiplication operations modulo m_1=2, m_2=3.

Therefore, two-dimensional IRB {(1,0),(1,1),(1,2)} generates a coordinate grid 2×3 over a toroidal surface with a common reference point (0,0):

(1,0)	(1,1)	(1,2)
(0,0)	(0,1)	(0,2)

The next we see result of multiplying IRB {(1,0),(1,1),(1,2)} by vector (1,2):

Here we see transformation IRB {(1,0), (1,1), (1,2)} into myself. Taking the same conversion for variants (*b*), (*c*), and (*d*), we finally obtain the next result: (*a*) × (1,2) ® (*a*); (*b*) × (1,2) ® (*b*); (*c*) × (1,2) ® (*d*); (*d*) × (1,2) ® (*c*).

Hence, the set of four 2-D IRBs {(*a*), (*b*), (*c*), (*d*)} form both two isomorphic (*a*, *b*), and two non-isomorphic (*c*, *d*) modifications of the 2-D IRB. We call this the cyclic two-dimensional IRB group. Note, that each of these variants makes it possible to obtain $m_1 \cdot m_2 = 2 \cdot 3 = 6$ varied 2−D IRBs.

Table 1 demonstrates optimized two-dimensional binary code, based on the 2-D IRB {(1,0), (1,1), (1,2)} with informative parameters *S*=7, *n*=3.

Table 1
Optimized two-dimensional binary code, based on the 2-D IRB {(1,0), (1,1), (1,2)} with informative parameters *S*=7, *n*=3

№	Vector	Digit weights of the 2-D code		
		(1,0)	(1,1)	(1,2)
1	(0,0)	0	1	1
2	(0,1)	1	1	0
3	(0,2)	1	0	1
4	(1,0)	1	0	0
5	(1,1)	0	1	0
6	(1,2)	0	0	1

Table 1 defines a two-dimensional binary code system as a torus surface coordinate grid $(n-1) \times n = 2 \times 3$ with two (t=2) circle axes m_1 =2, and m_2= 3. Here is an example of code system design, using the combinatorial optimization systems theory prospected from rotational symmetry of order seven (*S* =7). The example belongs design of an optimized data system processing two categories and three attributes concurrently (Table 2).

Table 2
Optimized data system processing two categories and three attributes concurrently.

№	Category		Digit weights of the 2-D code		
	1	2	(1,0)	(1,1)	(1,2)
1	0	0	0	1	1
2	0	1	1	1	0
3	0	2	1	0	1
4	1	0	1	0	0
5	1	1	0	1	0
6	1	2	0	0	1

Table 2 contains 6 binary 2-D (t = 2) 3- 3-digit (n = 3) combinations ($n^2 - n$ = 6) for coding two-dimensional (t = 2) data sets both with two (m_1 = 2) category of the first, and three (m_2 = 3) – the second attribute concurrently. More practical examples for combinatorial optimization of vector data processing are proposed in [16].

2.2.4 Multidimensional Ideal Ring Bundles

Multidimensional ideal ring bundles form a *t*-manifold coordinate system immersed in (*t*+1)-dimensional no real space without self-intersection of coordinate axes. A *t*-dimensional coordinate system (t > 2) with *t* axes is named the manifold coordinate system $m_1 \times m_2 \times \ldots \times m_t$. The principal property of coordinate grid $m_1 \cdot m_2 \cdot \ldots \cdot m_t$ over a *t*-manifold surface is *n*-stage sequence $\{K_1, K_2, \ldots, K_i, \ldots, K_n\}$, $K_1 = (k_{11}, k_{12}, \ldots, k_{1t})$, $K_2 = (k_{21}, k_{22}, \ldots, k_{2t})$, ..., $K_i = (k_{i1}, k_{i2}, \ldots, k_{it})$, ..., $K_n = (k_{n1}, k_{n2}, \ldots, k_{nt})$ of *t*-stage sub-sequences of the sequence, where we require a set modulo sums taking *t*- modulo (m_1, m_2 ,…., m_t) enumerates all coordinates of the *t*-manifold surface. This is perfect *t*-manifold coordinate system $m_1 \cdot m_2 \cdot \ldots \cdot m_t$ with information parameters *S*, *n*, m_i (i = 1, 2, …, *t*). It is a *t*-dimensional image surface involving spatially disjointed reference *t*-axes. A planar projection of *t*-dimensional manifold coordinate axes m_1, m_2, …, m_t for grid $m_1 \times m_2 \times \ldots \times m_t$ with common point illustrates Fig. 1.

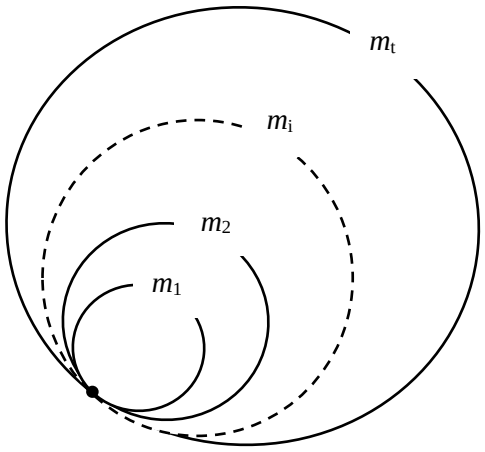

Fig.1: A planar projection of *t*-dimensional manifold coordinate axes m_1, m_2, …, m_t for grid $m_1 \times m_2 \times \ldots \times m_t$ with common point.

Here *S* is an order of spatial symmetry, *n*- number of *t*-stage sub-sequences of the *n*-sequence, and

number of basic attribute-categories subsets forming a complete set of *t*-dimensional vector data arrays. Hence, the t-dimensional IRB forms a manifold t-dimensional coordinate system. A *t*-dimensional perfect manifold coordinate system can be designed for configuring *t*-dimensional optimized control systems or CAD. Therefore, all information about the *t*-dimensional vector data array of sizes $m_1 \cdot m_2 \cdot \ldots \cdot m_t$ is embedded into the coordinate system.

3 Glory to Ukraine Stars Ensembles

Of very exciting property has been discovered in "Glory to Ukraine Star" (GUS) ensembles as a new type of spatial combinatorial configuration [16].
Graphic representation one of paired seven-pointed (n=7) GUS-configurations {(4,2), (0,2), (1,2), (0,4), (2,2), (3,2), (5,2), (4,2)} (black ring line) and {(4,2), (1,2), (2,2), (5,2), (3,2), (0,4), (0,2), (4,2)} (color broken line) are shown in Fig.2.

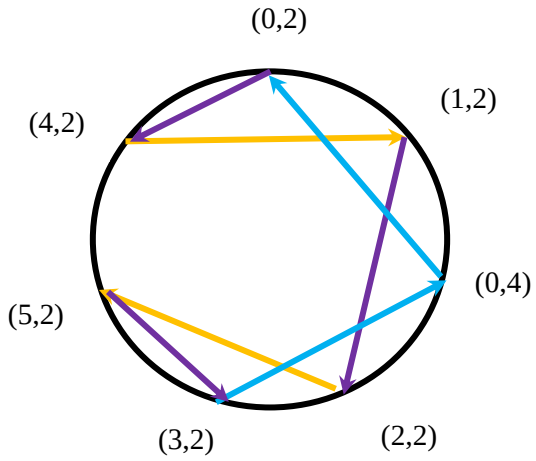

Fig.2: Graphic representation of paired seven-pointed (n=7) GUS-configurations {(4,2), (0,2), (1,2), (0,4), (2,2), (3,2), (5,2)} (black ring line) and {(4,2), (1,2), (2,2), (5,2), (3,2), (0,4), (0,2)} (color broken line).

The GUS-configuration {(4,2), (0,2), (1,2), (0,4), (2,2), (3,2), (5,2)} (black ring line) generates all $n(n-1)$= 42 two-dimensional ring sums, taking modulo (mod 6, mod 7) as follows:

1. (0,0) ≡ ((5,2)+(4,2)+(0,2)+(1,2)+(0,4)+(2,2));
2. (0,1) ≡ ((3,2) +(5,2)+(4,2)+(0,2));
3. (0,2) ≡ (0,2);
4. (0,3) ≡ ((1,2)+(0,4)+(2,2) +(3,2));
5. (0,4) ≡ (0,4);
6. (0,5) ≡ ((0,2)+ (1,2)+ (0,4)+ (2,2)+ (3,2));
7. (0,6) ≡ ((3,2)+(5,2)+(4,2));
8. (1,0) ≡ ((3,2)+(5,2)+(4,2)+(0,2)+(1,2)+(0,4));
9. (1,1) ≡ ((0,2)+ (1,2)+ (0,4));
10. (1,2) ≡ (1,2);
11. (1,3) ≡ ((3,2)+(5,2)+(4,2) +(0,2)+(1,2));
12. (1,4) ≡ (0,2)+(1,2));
13. (1,5) ≡ ((4,2)+ (0,2)+ (1,2)+(0,4)+ (2,2));
14. (1,6) ≡ ((1,2)+(0,4));
15. (2,0) ≡ ((0,4)+(2,2)+(3,2)+(5,2)+(4,2)+(0,2));
16. (2,1) ≡ ((2,2)+(3,2)+(5,2)+(4,2));
17. (2,2) ≡ (2,2);
18. (2,3) ≡ ((2,2)+(3,2)+(5,2)+(4,2)+(0,2));
19. (2,4) ≡ ((3,2)+(5,2));
20. (2,5) ≡ ((0,4)+(2,2)+(3,2)+(5,2)+(4,2));
21. (2,6) ≡ ((0,4)+(2,2));
22. (3,0) ≡ ((1,2)+(0,4)+(2,2) +(3,2)+(5,2)+(4,2));
23. (3,1) ≡ ((1,2)+(0,4)+ (2,2));
24. (3,2) ≡ (3,2);
25. (3,3) ≡ ((0,2)+ (1,2)+ (0,4)+ (2,2));
26. (3,4) ≡ ((5,2)+(4,2));
27. (3,5) ≡ ((2,2)+(3,2)+(5,2)+(4,2)+ (0,2)+ (1,2));
28. (3,6) ≡ ((5,2)+(4,2)+(0,2));
29. (4,0) ≡ ((4,2)+(0,2)+ (1,2)+ (0,4)+ (2,2)+ (3,2));
30. (4,1) ≡ ((5,2)+(4,2) +(0,2)+(1,2));
31. (4,2) ≡ (4,2);
32. (4,3) ≡ ((0,4)+(2,2)+(3,2)+(5,2));
33. (4,4) ≡ ((4,2)+(0,2));

34. (4,5) ≡
((5,2)+(4,2)+(0,2)+(1,2)+(0,4));
35. (4,6) ≡ ((2,2)+(3,2)+(5,2));
36. (5,0) ≡ ((0,2)+ (1,2)+ (0,4)+
(2,2)+(3,2)+(5,2));
37. (5,1) ≡ ((0,4)+ (2,2)+(3,2));
38. (5,2) ≡ (5,2);
39. (5,3) ≡ ((4,2)+(0,2)+(1,2)+(0,4));
40. (5,4) ≡ ((2,2)+(3,2));
41. (5,5) ≡ ((1,2)+ (0,4)+
(2,2)+(3,2)+(5,2));
42. (5,6) ≡ ((4,2)+(0,2)+(1,2));

The calculation procedures form $m_1 \times m_2 = 6\times7$ grid, embracing a two-dimensional (t=2) toroid surface as being a coordinate system, where each point node from (0,0) to (5,6) occurs exactly once (R=1).

The second of the paired GUS-configurations {(4,2), (1,2), (2,2), (5,2), (3,2), (0,4), (0,2)} (color broken line) forms the same set of sums, taking 2D modulo (mod 6, mod 7):

1. (0,0) ≡
((0,4)+(0,2)+(4,2)+(1,2)+(2,2)+(5,2));
2. (0,1) ≡ ((4,2)+(1,2)+(2,2)+(5,2));
3. (0,2) ≡ (0,2);
4. (0,3) ≡ ((0,2)+(4,2)+(1,2)+(2,2)+(5,2));
5. (0,4) ≡ (0,4);
6. (0,5) ≡ ((5,2)+(3,2)+(0,4)+(0,2)+(4,2));
7. (0,6) ≡ ((0,4)+(0,2));
8. (1,0) ≡
((5,2)+(3,2)+(0,4)+(0,2)+(4,2)+(1,2);
9. (1,1) ≡ ((0,2)+(4,2)+(1,2)+(2,2));
10. (1,2) ≡ (1,2);
11. (1,3) ≡ ((3,2)+(0,4)+(0,2)+(4,2));
12. (1,4) ≡ (2,2)+(5,2));
13. (1,5) ≡
((0,4)+(0,2)+(4,2)+(1,2)+(2,2));
14. (1,6) ≡((4,2)+(1,2)+(2,2));
15. (2,0) ≡ ((2,2)+
(5,2)+(3,2)+(0,4)+(0,2)+(4,2));
16. (2,1) ≡ ((5,2)+(3,2+(0,4));
17. (2,2) ≡ (2,2);
18. (2,3) ≡ ((5,2)+(3,2)+(0,4)+(0,2));
19. (2,4) ≡ ((5,2)+(3,2));
20. (2,5) ≡ (3,2)+(0,4)+(0,2)+(4,2)+(1,2);
……
42. (5,6) ≡ ((0,2)+(4,2)+(1,2)).

We observe either of the GUS-configurations {(4,2), (0,2), (1,2), (0,4), (2,2), (3,2), (5,2)} (black ring line) and {(4,2), (1,2), (2,2), (5,2), (3,2), (0,4), (0,2)} (color broken line) forms $m_1 \times m_2 = 6\times7$ grid, embracing toroid surface as 2-D coordinate system.

Here's another example of paired seven-pointed (n=7) GUS configurations.{(1,1), (1,3), (1,5), (1,0), (1,2), (1,4), (1,6)} (ring cycle), and {(1,1), (1,5), (1,2), (1,6), (1,3), (1,0), (1,4)} (star cycle) presents in Fig.3.

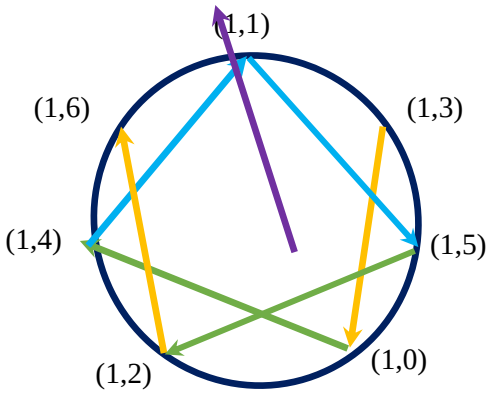

Fig.3: Paired seven-pointed (n=7) GUS-configurations, namely the {(1,0), (1,2), (1,4), (1,6), (1,1), (1,3), (1,5)} (ring cycle), and {(1,0), (1,4), (1,1), (1,5), (1,2), (1,6), (1,3)} (star cycle).

GUS-configuration {(1,1), (1,3), (1,5), (1,0), (1,2), (1,4), (1,6)} (ring cycle) forms the set of 2-D vector sums (clockwise), taking 2-D modulo (6, 7):

1. (0,0) ≡
((1,2)+(1,4)+(1,6)+(1,1)+(1,3)+(1,5));
2. (0,1) ≡ ((1,1)+(1,3)+ (1,5)+(1,0)+
(1,2)+(1,4));
3. (0,2) ≡
((1,0)+(1,2)+(1,4)+(1,6)+(1,1)+(1,3));
4. (0,3) ≡ ((1,6)+ (1,1)+
(1,3)+(1,5)+(1,0)+ (1,2));

5. (0,4) ≡ ((1,5)+(1,0)+ (1,2)+(1,4)+ (1,6)+(1,1));
……
……
41. (5,5) ≡ ((1,4)+(1,6)+ (1,1)+ (1,3)+(1,5);
42. (5,6) ≡ ((1,0)+ (1,2)+(1,4)+ (1,6)+(1,1)).

The second of the paired GUS configuration {(1,1), (1,5), (1,2), (1,6), (1,3), (1,0), (1,4)} (star cycle) forms the set of 2-D vector sums, taking modulo (mod 6, mod 7):

1. (0,0) ≡ ((1,4)+(1,1)+(1,5)+ (1,2)+(1,6)+(1,3));
2. (0,1) ≡ ((1,3)+ (1,0)+(1,4)+(1,1)+ (1,5)+(1,2));
3. (0,2) ≡ ((1,2)+(1,6)+(1,3) +(1,0)+(1,4)+(1,1));
4. (0,3) ≡ ((1,1)+(1,5)+ (1,2)+(1,6)+(1,3)+(1,0));
5. (0,4) ≡ ((1,0)+(1,4)+ (1,1)+(1,5)+ (1,2)+(1,6));
……
……
41. (5,5) ≡ ((1,0)+(1,4)+ (1,1)+ (1,5)+(1,2);
42. (5,6) ≡ ((1,3)+ (1,0)+(1,4)+ (1,1)+(1,5)).

Each of the paired seven-pointed (n=7) GUS-configurations, {(1,1), (1,3), (1,5), (1,0), (1,2), (1,4), (1,6)} (ring cycle), and {(1,1), (1,5), (1,2), (1,6), (1,3), (1,0), (1,4)} (star cycle) forms $m_1 \times m_2 = 6\times7$ grid, embracing two-dimensional (t=2) toroid surface as coordinate system exactly once (R=1).

The underlying examples of paired seven-pointed (n=7) GUS-configurations evident that either of the combinatorial configurations {(4,2), (0,2), (1,2), (0,4), (2,2), (3,2), (5,2)}, {(4,2), (1,2), (2,2), (5,2), (3,2), (0,4), (0,2)}, {(1,1), (1,3), (1,5), (1,0), (1,2), (1,4), (1,6)}, {(1,1), (1,5), (1,2), (1,6), (1,3), (1,0), (1,4)} forms complete coordinate system $m_1 \times m_2 = 6\times7$ over toroid surface.

A graphic representation of a set of paired seven-pointed (n=7) GUS ensembles is illustrated (Fig.4).

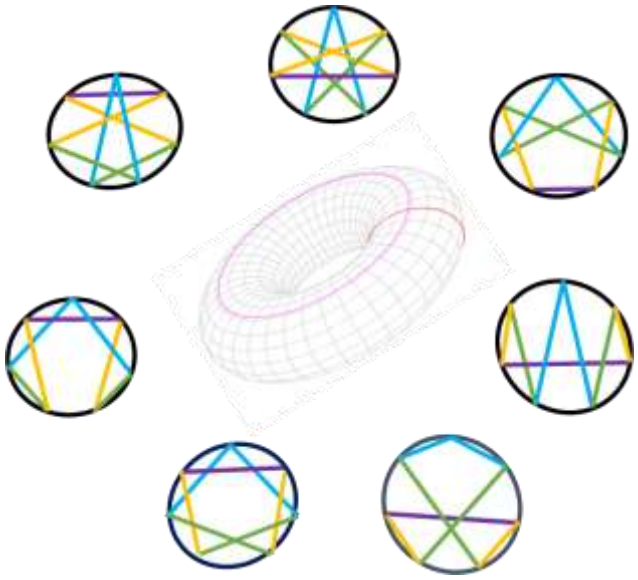

Fig. 4: Graphic representation of a set of paired seven-pointed (n=7) GUS ensembles.

The cardinal number P of paired 2-D GUS configurations depending on the n-pointing cyclic structures with $m_1 \times m_2$ grid sizes for n = 2,3,…7 is given in Table 3.

Table 3
The cardinal number P of paired 2-D GUS configurations depending on the n-pointing cyclic structures with $m_1 \times m_2$ grid sizes for n = 2,3,…7

n	Grid sizes $m_1 \times m_2$	P
2	1×2	1
3	2×3	4
4	3×4	24
5	4×5, 3×7	272
6	5×6, 3×10	256
7	6×7, 3×14	360

Table 3 shows an increasing number of paired 2-D GUS configurations, arranged by n-pointing cyclic structures.

4 Conclusion

The theory of combinatorial optimization systems, explored through the lens of rotational symmetry,

offers a novel way to conceptualize engineering devices and technical systems in an optimized manner. This approach allows for the optimization to be integrated into the model itself, thereby enabling the configuration of systems with fewer elements than currently used, while still maintaining or even improving other characteristics of the system. The theoretical connection between cyclic groups and IRBs presents significant opportunities for the advancement of systems theory in configuring innovative devices and process engineering. This is due to the exceptional mathematical properties and structural perfection of IRBs. The use of optimized perfect manifold coordinate systems in information technologies offers new conceptual techniques to improve the quality of technology and management systems. This includes improving the transmission and compression of vector data and ensuring the reliability of vector data coding and processing using a minimized basis of manifold coordinates. The essence of the technology is processing vector information in the database of manifold coordinate systems, where the basis is a set of coordinates smaller than the total number of coordinates of this coordinate system, which generates it by adding the latter. The theoretical connection between cyclic groups and IRBs presents significant opportunities for the advancement of systems theory in configuring innovative devices and process engineering. This is due to the exceptional mathematical properties and structural perfection of IRBs. The exceptional mathematical properties and structural perfection of IRBs create significant opportunities for the advancement of systems theory in configuring innovative devices and process engineering through their theoretical connection with cyclic groups. Multidimensional systems engineering can be improved by researching combinatorial optimization systems theory, with a focus on rotational symmetry. This improvement can lead to better quality indices such as information capacity, reliability, transmission speed, positioning precision, and the ability to reproduce the maximum number of combinatorial varieties in the system with a limited number of elements and bonds. The GUS combinatorial configurations have remarkable properties and structural perfection, which can be utilized for direct applications in information and computational technologies, telecommunications, radio and electronic engineering, radio physics, and other engineering areas, as well as in education. By using these design techniques, you can configure optimum two- and multidimensional vector data processing, using innovative methods based on the underlying combinatorial models, which offers ample scope for progress in systems engineering, cybernetics, computational and applied mathematics, and industrial informatics.

Declaration of Generative AI and AI-assisted technologies in the writing process

During the preparation of this work the author used GRAMMARLY in order to IMPROVE GRAMMAR. After using this tool/service, the author reviewed and edited the content as needed and takes full responsibility for the content of the publication.

References:

[1] Bernhard Korte, Jens Vygen, "Combinatorial Optimization," Springer Berlin, Heidelberg, 2018, 698 p. https://doi.org/10.1007/978-3-662-56039-6

[2] M. Jr. Hall, "Combinatorial Theory," 2nd Edition, Wiley-Interscience, 1998, 464 p.

[3] Steingrímsson, Einar; "Some open problems on permutation patterns", *Surveys in combinatorics* 2013, London Math. Soc. Lecture Note Ser., Vol. 409, Cambridge Univ. Press, Cambridge, 2013, pp. 239–263. DOI: 10.1007/978-1-4612-0617-0

[4] N.R.Bose, *Applied Multidimensional Systems Theory*, Springer Int. Publishing AG, 2017, Pennsylvania State University, State College, PA.

[5] A Oussous, FZ Benjelloun, and AA Lahcen. Big Data technologies: A survey… - *Journal of King Saud* …, 2018 - Elsevier

[6] Renu Aabharwal, and Shah Jahan Miah," A new theoretical understanding of big data analytics capabilities." Journal of Big Data 8, 159 (2021), https://doi.org/10.1186/s40537-021-00543-6

[7] Shah J Miah, Edwin Camilleri, and H.Quan Vu, "Big Data in healthcare research: a survey study." Journal of Computer Information Systems. Volume 62, 2022- Issue 3, 480-492. https://doi.org/10.1080/08874417.2020.1858727

[8] Soori, M.; Arezoo, B.; Dastres, R. Artificial Intelligence, Machine Learning and Deep Learning in Advanced Robotics, a Review. *Cogn. Robot.* 2023, *3*, 54–70.

[9] Licardo, J.T.; Domjan, M.; Orehovački, T. Intelligent Robotics—A Systematic Review of Emerging Technologies and Trends. *Electronics* 2024, *13*, 542.

[10] Huixu Dong**,** Yuanzheng Ge**,** Rui Zhou, and Hongyan Wang,"An Improved Sorting Algorithm for Periodic PRI Signals Based on Congruence Transform,"*Symmetry* 2024, 16(4), 398; https://doi.org/10.3390/sym16040398

[11] Kang, K.; Zhang, Y.X.; Guo, W.P. Key Radar Signal Sorting and Recognition Method Based on Clustering Combined with PRI Transform Algorithm. *J. Artif. Intell. Technol.* 2022, *2*, 62–68.

[12] Labbaf, N.; Oskouei, H.D.; Abedi, M.R. Robust DOA estimation in a uniform circular array antenna with errors and unknown parameters using deep learning. *IEEE Trans. Green Commun. Netw.* 2023, *7*, 2143–2152

[13] Huixu Dong**,** Yuanzheng Ge**,** Rui Zhou, and Hongyan Wang, "An Improved Sorting Algorithm for Periodic PRI Signals Based on Congruence Transform,"*Symmetry* 2024, 16(4), 398; https://doi.org/10.3390/sym16040398

[14] Dong, H.; Wang, X.; Qi, X.; Wang, C. An Algorithm for Sorting Staggered PRI Signals Based on the Congruence Transform. *Electronics* 2023, *12*, 2888.

[15] Huawei Huang, Weisha Kong, and Ting Xu, "Asymmetric Cryptography Based on the Tropical Jones Matrix," *Symmetry* 2024, 16(4), 440; https://doi.org/10.3390/sym16040440

[16] V.Riznyk, Optimum Vector Information Technologies Based on the Multidimensional Combinatorial Configurations. *International Journal of Computational and Applied Mathematics & Computer Science*, Vol. 3, 2023, pp.104-112.

[17] Simone Fiori,"Manifold Calculus in System Theory and Control – Fundamentals and First-Order Systems." *Symmetry* 2021, 13(11), 2092; https://doi.org/10.3390/sym13112092

[18] Igor Kriz, Sophie Kriz, *Introduction to Algebraic Geometry*, Birkhäuser Cham, 2021, 470 p. https://doi.org/10.1007/978-3-030-62644-0

[19] Claudia Salera, Camilla Vallebella**,**Marco Iosa, and Anna Pecchinenda, "Fibonacci Sequence and the Golden Ratio". *Symmetry* 2024, 16(3), 333; https://doi.org/10.3390/sym16030333

[20] Hall, Graham (2004). Symmetries and Curvature Structure in General Relativity (World Scientific Lecture Notes in Physics). Singapore: *World Scientific*. ISBN 981-02-1051-5

Contribution of Individual Authors to the Creation of a Scientific Article (Ghostwriting Policy)

Please visit Contributor Roles Taxonomy (CRediT) that contains several roles:

www.wseas.org/multimedia/contributor-role-instruction.pdf

The authors equally contributed in the present research, at all stages from the formulation of the problem to the final findings and solution.

Sources of Funding for Research Presented in a Scientific Article or Scientific Article Itself

No funding was received for conducting this study.

Conflict of Interest

The authors have no conflicts of interest to declare that are relevant to the content of this article.